ARTICLES

Journal of Semiconductors
(2024) 45, 102101
doi: 10.1088/1674-4926/24030002

Impact of strain relaxation on the growth rate of heteroepitaxial germanium tin binary alloy

Pedram Jahandar† and Maksym Myronov

Department of Physics, University of Warwick, Coventry, CV4 7AL, United Kingdom

Abstract: The growth of high-quality germanium tin ($Ge_{1-y}Sn_y$) binary alloys on a Si substrate using chemical vapor deposition (CVD) techniques holds immense potential for advancing electronics and optoelectronics applications, including the development of efficient and low-cost mid-infrared detectors and light sources. However, achieving precise control over the Sn concentration and strain relaxation of the $Ge_{1-y}Sn_y$ epilayer, which directly influence its optical and electrical properties, remain a significant challenge. In this research, the effect of strain relaxation on the growth rate of $Ge_{1-y}Sn_y$ epilayers, with Sn concentration >11at.%, is investigated. It is successfully demonstrated that the growth rate slows down by ~55% due to strain relaxation after passing its critical thickness, which suggests a reduction in the incorporation of Ge into $Ge_{1-y}Sn_y$ growing layers. Despite the increase in Sn concentration as a result of the decrease in the growth rate, it has been found that the Sn incorporation rate into $Ge_{1-y}Sn_y$ growing layers has also decreased due to strain relaxation. Such valuable insights could offer a foundation for the development of innovative growth techniques aimed at achieving high-quality $Ge_{1-y}Sn_y$ epilayers with tuned Sn concentration and strain relaxation.

Key words: GeSn; germanium tin; strain relaxation; group Ⅳ semiconductor; chemical vapour deposition; CVD

Citation: P Jahandar and M Myronov, Impact of strain relaxation on the growth rate of heteroepitaxial germanium tin binary alloy[J]. *J. Semicond.*, 2024, 45(10), 102101. https://doi.org/10.1088/1674-4926/24030002

1. Introduction

The fundamental electronic energy bandgap is the most important parameter of a semiconductor, upon which other electronic and optical properties sensitively depend. It is crucial to carefully control the bandgap to optimise the performance of semiconductor devices. Bandgap engineering can be achieved by changing compositions in a semiconductor alloy system[1]. The field of bandgap engineering was significantly expanded with the introduction of epitaxial growth techniques[2]. Epitaxy refers to growth of crystalline layer, known as epitaxial layer, on top of a crystalline substrate with the same orientation. In this technique, large stresses in epitaxial layers are generated because of lattice constant mismatch between epitaxial layer and substrate[3]. The strain in epitaxial layer provides an additional design flexibility for electronic band structure engineering. However, such flexibility is influenced and limited to a critical thickness of epitaxial layer, where strain starts to relieve due to formed defects as a consequence of strain relaxation[3]. For example, if lattice constant of epitaxial layer significantly depends on its composition, appropriate composition could lead to significant strain energy and so large reduction in h_c into an undesirable value. When growing a material with the same crystal structure with a different lattice constant from the substrate or buffer layer (referred to as a virtual substrate (VS)), the grown material either has a tensile strain or a compressive strain. In the case of $Ge_{1-y}Sn_y$ grown on Ge-VS (or Si substrate), the grown $Ge_{1-y}Sn_y$ epilayer will have a compressive strain because its lattice constant is larger than that of Ge-VS (or Si substrate). If the grown $Ge_{1-y}Sn_y$ has exactly the same inner plane (in-plane) lattice parameter as its Ge-VS (or Si substrate) but a larger outer plane (out-of-plane) lattice parameter, it is referred to as a fully strained $Ge_{1-y}Sn_y$. Fully strained $Ge_{1-y}Sn_y$ epilayer can be grown up to a certain thickness, so called critical thickness h_c, which mainly depends on Sn concentration (y). Above h_c, $Ge_{1-y}Sn_y$ epilayer gradually begins to relax the compressive strain.

The lattice constant of $Ge_{1-y}Sn_y$ is larger than that of Ge; however, this lattice constant closely depends on the Sn concentration in $Ge_{1-y}Sn_y$, especially in samples that are not fully strained. As the Sn concentration (y) in the $Ge_{1-y}Sn_y$ binary alloy increases, its lattice volume is expected to increase. The growth of high quality $Ge_{1-y}Sn_y$, in which segregation and precipitation is controlled, directly on Si substrate using CVD is very challenging due to its large lattice mismatch. To overcome this challenge, a high quality relaxed Ge buffer, which has a larger lattice constant than Si, can be grown on Si substrate and used as an intermediate layer, VS, to reduce the effective lattice mismatch. The strain is a key parameter that influences the physical, optical, and electrical properties of the $Ge_{1-y}Sn_y$ epilayer. For example, it has been suggested that tensile and compressive strain reduce and increase the required Sn concentration to achieve indirect-to-direct bandgap transition, respectively[4, 5]. In addition to Sn concentration, it is possible to adjust carrier mobility[6, 7] and band structure[4, 8] of the epilayer by modifying the strain in the $Ge_{1-y}Sn_y$ epilayer. Therefore, it is essential to fully understand the strain relaxation of $Ge_{1-y}Sn_y$ epilayers.

Theoretically, it should be possible to tune the room temperature energy bandgap of $Ge_{1-y}Sn_y$ alloy from 0.66 eV

Correspondence to: P Jahandar, P.Jahandar@warwick.ac.uk
Received 4 MARCH 2024; Revised 30 APRIL 2024.

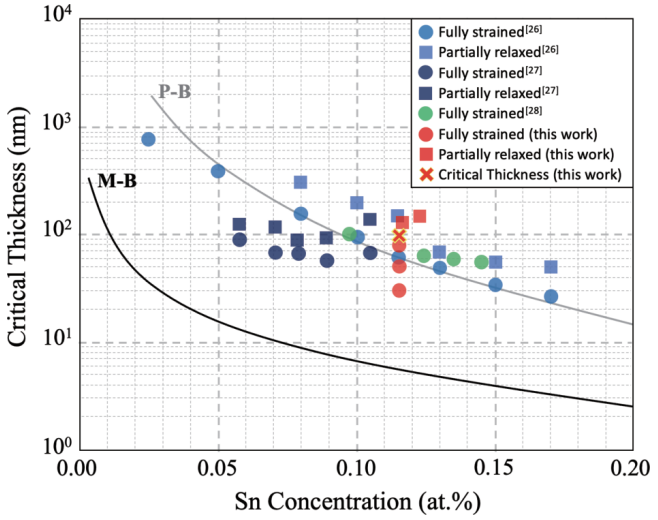

Fig. 1. (Colour online) Theoretical calculations of h_c for $Ge_{1-y}Sn_y$ films grown on Si substrate via a relaxed Ge-VS using the People Bean (P–B) model and the Matthew Blakeslee (M–B) model[13]. Experimental data collected from this work as well as previous research are included[14–16].

down to 0.0 eV by modifying the Sn concentration in $Ge_{1-y}Sn_y$[9, 10]. Ge is a group Ⅳ semiconductor with an indirect bandgap and an energy difference of 0.66 eV between the lowest conduction band minimum, *L*-point, and the highest valence band maximum, *Γ*-point, at room temperature[5]. As y increases in $Ge_{1-y}Sn_y$, the *L*-valleys diminishes slower than the *Γ*-valley as a consequence of $E_{g\Gamma,Ge} - E_{g\Gamma,\alpha Sn} > E_{gL,Ge} - E_{gL,\alpha Sn}$, suggesting an indirect-to-direct bandgap transition for a certain[5]. It has been shown that bandgap energy decreases as a result of tensile biaxial strain in $Ge_{1-y}Sn_y$, as the effect of strain is significantly higher in direct gap than indirect[11, 12]. The achievement of direct bandgap $Ge_{1-y}Sn_y$ depends strongly on its strain relaxation, for instance, for compressive strained $Ge_{1-y}Sn_y$, higher Sn concentration is required for an indirect-to-direct bandgap transition than tensile strained $Ge_{1-y}Sn_y$[5].

Theoretical investigations have shown that biaxial strain can significantly affect the bandgap structure of $Ge_{1-y}Sn_y$. Specifically, it has been suggested that tensile and compressive strains can respectively decrease and increase the required Sn concentration to achieve an indirect-to-direct bandgap transition in $Ge_{1-y}Sn_y$[4]. Tensile strained $Ge_{1-y}Sn_y$ can be grown on partially or fully relaxed $Ge_{1-y}Sn_y$ with a different Sn concentration[17–20], while compressive strained $Ge_{1-y}Sn_y$ can be grown on Si via Ge-VS[21, 22]. Recent predictions indicate that an indirect-to-direct bandgap transition in $Ge_{1-y}Sn_y$ can be achieved with a Sn concentration ranging from 6 at.% to 11 at.%[4, 23–27].

Therefore, it is crucial to have a comprehensive understanding of the impact of strain relaxation on the growth rate of $Ge_{1-y}Sn_y$ epilayers, in addition to understanding its critical thickness and Sn concentration, to facilitate the development of optoelectronic devices. As seen in Fig. 1, many studies have been carried out to estimate critical thicknesses and the effect of strain relaxation on Sn concentration as well as quality of epilayers. However, no study has been done to investigate the effect of strain relaxation on growth rate, which is presented in this research.

2. Experimental techniques

2.1. Heteroepitaxy of $Ge_{1-y}Sn_y$ epilayers

In this research, all crystalline materials were grown using the ASM Epsilon 2000 system. It is one of the most common epitaxy tools in semiconductor manufacturing, having been used for about three decades to grow Si, Ge, $Si_{1-x}Ge_x$, $Si_{1-x}C_x$ and many other group Ⅳ semiconductors. It is a horizontal flow, load-locked, and single wafer reduced-pressure chemical vapour deposition (RP-CVD) tool developed for high-volume semiconductor production in various epitaxy applications. The Si wafer is mounted on a graphite susceptor coated with silicon carbide, which is located in a quartz chamber with a cold wall. During the process, infrared (IR) lamps are responsible for heating the susceptor and the wafer, ones placed on the bottom and the others on the top of the quartz chamber. To control growth at low temperatures, thermocouples embedded in the susceptor are used.

All $Ge_{1-y}Sn_y$ epilayers were grown on 100 mm Si (001) wafers via 0.6 μm thick relaxed Ge virtual substrate. By growing thick enough Ge buffer layer on top of Si (001), strain relaxation within the Ge buffer layer is achieved and so effective lattice mismatch between Si substrate and $Ge_{1-y}Sn_y$ decreases from ~20 % to ~15 %[5]. Tin-tetrachloride ($SnCl_4$) was used in combination with germane (GeH_4) with H_2 as a carrier gas and chamber pressure controller. All growth was carried out at 260 °C and 500 Torr.

2.2. Measurements of Sn concentration

The Sn concentration of each $Ge_{1-y}Sn_y$ epilayer was measured using high-resolution X-ray diffraction (HR-XRD). HR-XRD ω–2θ coupled scan, symmetric and asymmetric reciprocal space maps (RSMs) were used, alongside with the modified Vegard's law to measure the Sn concentrations. The Vegard's law used in this research is:

$$a_0^{Ge_{1-y}Sn_y} = (1-y)\cdot a_0^{Ge} + y\cdot a_0^{Sn} + y(1-y)\cdot b^{GeSn}, \quad (1)$$

where a_0 is the relaxed lattice constant of each crystal, and b^{GeSn} is the bowing parameter. The bowing parameter (b^{GeSn}) used in this research is 0.041 Å[15] according to the latest agreed studies and relaxed lattice constant, a_0 is 5.6579 and 6.4892 Å for Ge and Sn, respectively[5]. The lattice constant of each epilayer was calculated from the in and out of plane lattice parameters obtained from RSMs.

3. Results and discussion

3.1. Sn concentration, critical thickness h_c and surface morphology of $Ge_{1-y}Sn_y$ epilayers

In this work, the h_c value of $Ge_{1-y}Sn_y$, which represents the thickness where strain relaxation begins in the epilayer, is initially investigated. The Sn concentration of 11.6 at.% was obtained for the fully strained $Ge_{1-y}Sn_y$ epilayers. The Sn concentration for each sample was measured from RSMs using the modified Vegard's law. As seen in Fig. 2(a), the thickness fringes around $Ge_{1-y}Sn_y$ peak in HR-XRD ω–2θ coupled scan for the $Ge_{1-y}Sn_y$ epilayer grown for 10 min began to disappear. This indicates the beginning of strain relaxation in the $Ge_{1-y}Sn_y$ epilayer. The thickness of the $Ge_{1-y}Sn_y$ epilayer grown for 10 min was measured using X-TEM to be 95 nm.

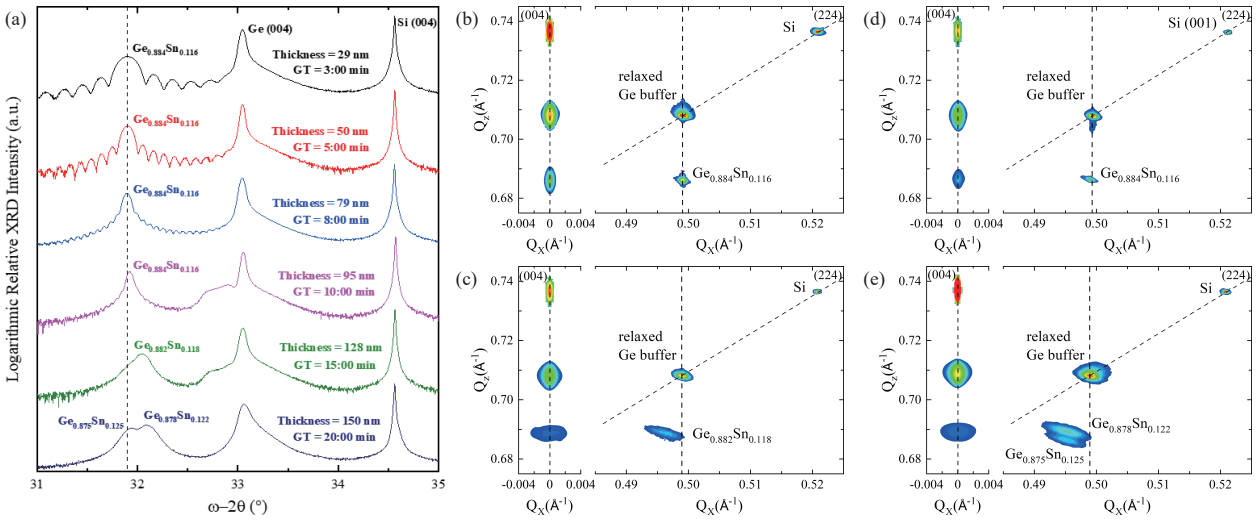

Fig. 2. (Colour online) (a) HR-XRD ω–2θ coupled scans for $Ge_{1-y}Sn_y$ epilayers grown with different growth times on Si (001) via Ge-VS. Symmetric and asymmetric RSMs for $Ge_{1-y}Sn_y$ grown with different growth times on Si (001) via Ge-VS of (b) 79 nm thick $Ge_{0.884}Sn_{0.116}$ grown for 8 min, (c) 95 nm thick $Ge_{0.884}Sn_{0.116}$ grown for 10 min, (d) 128 nm thick $Ge_{0.882}Sn_{0.118}$ grown for 15 min, and (e) 150 nm thick $Ge_{0.878}Sn_{0.122}$ grown for 20 min. The Sn concentration for each of these samples was measured from RSMs and using the modified Vegard's law. The thicknesses of these epilayers are measured using either thickness fringes appeared in their HR-XRD ω–2θ coupled scans or X-TEM images, as shown in the example in Fig. 3(a).

This shows that the h_c value for $Ge_{1-y}Sn_y$ epilayers grown under the given CVD growth conditions is approximately ~95 nm which agrees with previous studies shown in Fig. 1.

When comparing the HR-XRD ω–2θ coupled scans of the $Ge_{1-y}Sn_y$ epilayers shown in Fig. 2(a), it becomes evident that as more strain relaxation is achieved, the $Ge_{1-y}Sn_y$ peak in the HR-XRD ω–2θ coupled scan begins to shift to the right. This shift is solely due to strain relaxation within the layers of $Ge_{1-y}Sn_y$ and not to a reduction in Sn concentration. This is demonstrated when measuring the Sn concentration using XRD RSMs.

As shown in Fig. 2(b), the $Ge_{1-y}Sn_y$ grown for 8 min is fully strained, and its peak appeared exactly under the relaxed Ge-VS in the asymmetric RSM. However, for the $Ge_{1-y}Sn_y$ grown for 10 min, as shown in Fig. 2(c), the $Ge_{1-y}Sn_y$ peak in the asymmetric RSM is slightly shifted to the left, indicating the appearance of strain relaxation in the $Ge_{1-y}Sn_y$ layers. In addition, for the $Ge_{1-y}Sn_y$ grown for 15 min, as shown in Fig. 2(d), the $Ge_{1-y}Sn_y$ peak in the asymmetric RSM is significantly shifted to the left, indicating a greater degree of strain relaxation in the $Ge_{1-y}Sn_y$ layers compared to the previous epilayer, which was grown for only 10 min. As shown in Fig. 2(d), the Sn concentration of the $Ge_{1-y}Sn_y$ epilayer grown under the same CVD growth conditions has indeed increased due to strain relaxation. The $Ge_{1-y}Sn_y$ epilayer grown for 15 min has 0.2 at.% more Sn concentration than the fully strained $Ge_{1-y}Sn_y$ epilayer grown for 8 min. For the $Ge_{1-y}Sn_y$ epilayer grown for 10 min, no change in Sn concentration was observed as the epilayer has just begun to relax at the h_c of ~95 nm.

An additional $Ge_{1-y}Sn_y$ epilayer was also grown for 15 min under the same growth conditions, indicating a relaxation of strain in the epilayer. The thickness of this epilayer is also measured using X-TEM. As seen in Fig. 2(a), an additional peak is observed next to each of the HR-XRD ω–2θ coupled scans of $Ge_{1-y}Sn_y$ epilayers (with apparent strain relaxation), which were grown for 10 and 15 min. It should be noted that shoulders on the left side of the Ge peak in HR-XRD ω–2θ coupled scans are normally considered to be due to polycrystalline $Ge_{1-y}Sn_y$ or $Ge_{1-y}Sn_y$ with very low Sn concentration (around Sn solubility in Ge). Nevertheless, as can be seen in Fig. 2(a), such peaks or shoulders are not present in HR-XRD ω–2θ coupled scans of fully strained $Ge_{1-y}Sn_y$ epilayers grown under the same CVD conditions. The apparent shoulders are presumably due to Sn segregation, especially considering they are not evident for fully strained $Ge_{1-y}Sn_y$ epilayers. As such, the shoulder does not appear in the HR-XRD ω–2θ coupled scan of the 150 nm thick $Ge_{0.878}Sn_{0.122}$. It may depend on the area of the epilayer scanned; thus, some areas on the wafers have no Sn segregation.

A thicker $Ge_{1-y}Sn_y$ epilayer was grown for 20 min under the same growth conditions. Symmetric and asymmetric RSMs of the heterostructure are shown in Fig. 2(e). At first glance, two $Ge_{1-y}Sn_y$ peaks in the asymmetric RSM can be noticed. Before discussing the double $Ge_{1-y}Sn_y$ peaks, it is important to note that both $Ge_{1-y}Sn_y$ peaks are more relaxed (shifted more to the left in asymmetric RSM) than the $Ge_{1-y}Sn_y$ peak in asymmetric RSM of thinner $Ge_{1-y}Sn_y$ epilayers. In addition, both $Ge_{1-y}Sn_y$ peaks indicate higher Sn concentrations than thinner $Ge_{1-y}Sn_y$, as shown in Fig. 2, confirming an increase in Sn concentration due to strain relaxation. In Fig. 3(a), high resolution X-TEM of $Ge_{0.878}Sn_{0.122}$ is given which shows thickness and smooth surface of the epilayer.

A summary of the relationship between thickness, Sn concentration and total growth rate of $Ge_{1-y}Sn_y$ epilayers is shown in Fig. 3(b). For the $Ge_{1-y}Sn_y$ epilayer with growth time of 20 min (150 nm thick $Ge_{1-y}Sn_y$ epilayer), only one peak is included (the one with lower Sn concentration). It should be noted that this summary is only valid for $Ge_{1-y}Sn_y$ epilayers grown under the same CVD conditions using the same precursors and respective partial pressures. This is because each of these CVD conditions can influence lattice diffusion and thus h_c. For example, as the growth temperature decreases, lattice diffusion is minimised which may increases the h_c.

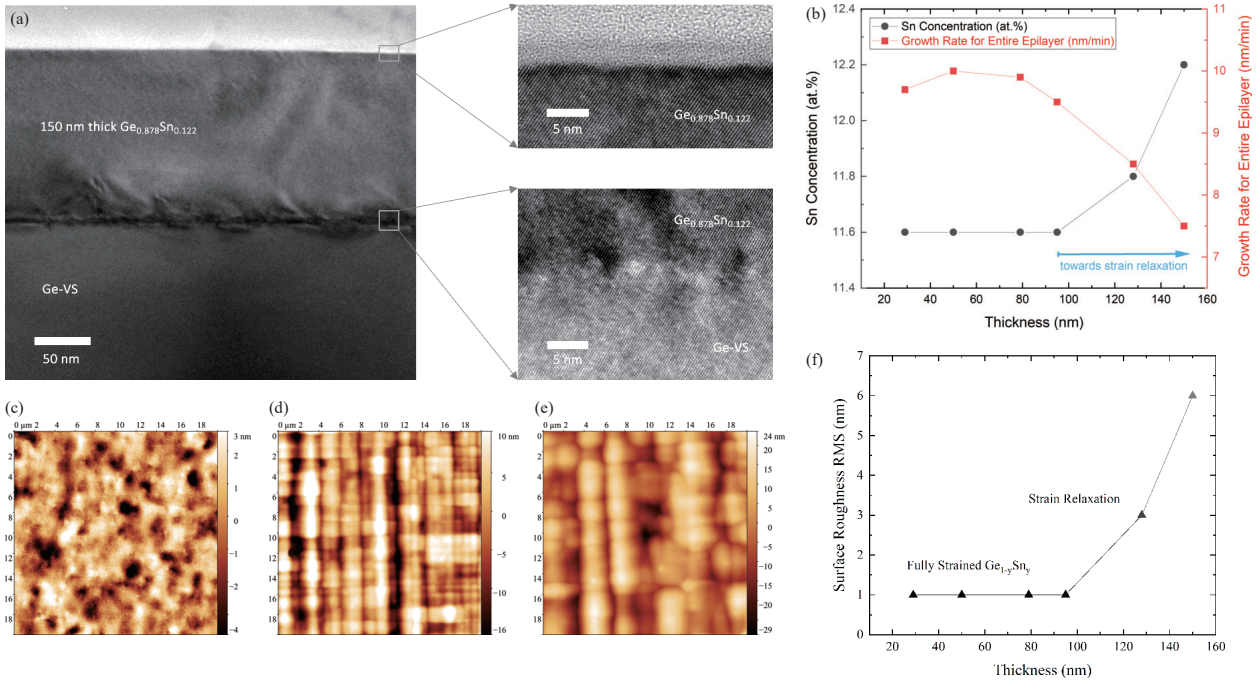

Fig. 3. (Colour online) (a) X-TEM image of 150 nm thick $Ge_{0.878}Sn_{0.122}$ grown on Ge-VS. The high resolution lattice resolved X-TEM micrographs of $Ge_{0.878}Sn_{0.122}$/Ge-VS interface as well as surface of $Ge_{0.878}Sn_{0.122}$ epilayer are presented. (b) Relationship between thickness, Sn concentration and total growth rate of $Ge_{1-y}Sn_y$ epilayers. (c) AFM scan of 95 nm thick $Ge_{0.884}Sn_{0.116}$. (d) AFM scan of 128 nm thick $Ge_{0.882}Sn_{0.118}$. (e) AFM scan of 150 nm thick $Ge_{0.878}Sn_{0.122}$. (f) Surface roughness (RMS) of $Ge_{1-y}Sn_y$ epilayers with different thicknesses. Surface roughness increased with the increase in thickness (growth time), particularly after the critical thickness of ~95 nm.

Another example is the Sn concentration itself: as the Sn concentration in the $Ge_{1-y}Sn_y$ epilayer increases, the h_c decreases, so the epilayer strain relaxation is achieved more quickly.

Moreover, if the thickness of the $Ge_{1-y}Sn_y$ epilayer is greater than h_c, misfit dislocations can form at the two ends[28]. These dislocations could create a loop so that the two ends can join or thread onto the surface, which could potentially restrict applications of relaxed $Ge_{1-y}Sn_y$[6, 29]. Examples of AFM scans of the epilayers with various thicknesses are provided in Figs. 3(c)–3(e). The surface roughness in terms of RMS for all $Ge_{1-y}Sn_y$ epilayers grown in this study is shown in Fig. 3(f). It is evident that the surface roughness remained low for all fully strained $Ge_{1-y}Sn_y$, and as soon as a h_c of ~95 nm was reached (at growth time of ~10 min), the surface roughness began to increase. This could be due to Sn segregation, which may be a consequence of strain relaxation[30].

It is important to discuss the reasons for the appearance of two $Ge_{1-y}Sn_y$ peaks (as can be seen in Fig. 2(e)) in asymmetric RSM of $Ge_{1-y}Sn_y$ epilayer grown for 20 min. The justification for this behaviour is as follows: the second peak, which indicates that $Ge_{1-y}Sn_y$ layers with a slightly higher Sn concentration can be grown when a certain strain relaxation is achieved. The Sn concentration increases gradually and steadily as the layers relax (as the thickness of the epilayer increases) until a certain point. After this certain point, there is a sudden transition to Sn concentration, because the top layers (which now act as an intermediate substrate) allow $Ge_{1-y}Sn_y$ to grow with such a higher Sn concentration.

3.2. Effect of strain relaxation on growth rate

In this section, the effect of strain relaxation on the growth rate of $Ge_{1-y}Sn_y$ epilayers is investigated. As shown in Fig. 3(b), the growth rate of $Ge_{1-y}Sn_y$ epilayers decreases with increasing thickness. The growth rates shown in Fig. 3(b) are the growth rates for the entire $Ge_{1-y}Sn_y$ epilayers. To understand the effect of strain relaxation on growth rate, it is therefore necessary to investigate the relationship between growth rate and thickness of $Ge_{1-y}Sn_y$ epilayers.

As shown in Fig. 4(a), the average growth rate for fully strain $Ge_{1-y}Sn_y$ grown up to 10 min under the given CVD conditions was 9.8 nm/min. We assumed that for partially relaxed $Ge_{1-y}Sn_y$ epilayers, which were grown for 15 and 20 min, the growth rate for the initial 10 min was the same as the growth rate for fully strained $Ge_{1-y}Sn_y$ epilayers. Based on this assumption, the average growth rate from 10 to 15 min was measured at 6.1 nm/min and the average growth rate from 15 to 20 min was measured at 4.4 nm/min. These growth rates were calculated by growing $Ge_{1-y}Sn_y$ with different growth times.

Considering the average growth rates of the epilayers depending on their thickness as shown in Fig. 4(a), it is possible to understand the effect of strain relaxation on growth rates. As shown in Fig. 4(b), a straight line (orange colour) is fitted to the data, representing the average growth rate at the given thickness of the $Ge_{1-y}Sn_y$ epilayer. For thicknesses below the h_c, in which all $Ge_{1-y}Sn_y$ epilayers are fully strained, the growth rate is assumed to remain constant. Therefore, a straight horizontal line was fitted to those epilayers with thickness of up to h_c. The epilayers with thickness of above h_c are partially relaxed and their degree of relaxation is discussed in the next Section. It is also evident that the rate of suppression in the average growth rate is at its highest level just after the $Ge_{1-y}Sn_y$ epilayer passes the h_c, and the rate of reduction in the average growth rate gradually decreases as the thickness of the epilayer increases.

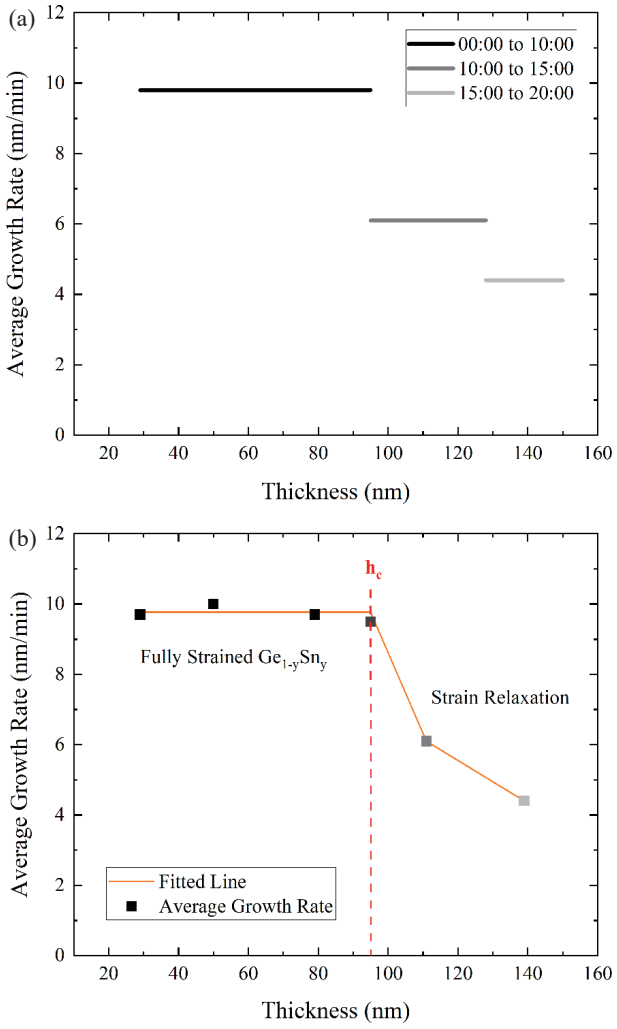

Fig. 4. (Colour online) (a) Average growth rate (nm/min) at the given thickness (nm) of the $Ge_{1-y}Sn_y$ and its corresponding growth time (min). As the thickness of the $Ge_{1-y}Sn_y$ increases, the growth rate decreases. (b) Actual data points collected experimentally for average growth rate (nm/min).

The in-plane and out-of-plane strain of $Ge_{1-y}Sn_y$ epilayers grown were estimated using the following equations:

$$\text{Strain}_{\text{in-plane}} = \frac{a_{\parallel}^{\text{GeSn}} - a_0^{\text{GeSn}}}{a_0^{\text{GeSn}}}, \quad (2)$$

$$\text{Strain}_{\text{out-of-plane}} = \frac{a_{\perp}^{\text{GeSn}} - a_0^{\text{GeSn}}}{a_0^{\text{GeSn}}}, \quad (3)$$

where $a_{\parallel}$ and $a_{\perp}$ are in-plane and out-of-plane of the lattice respectively. Additionally, a_0^{GeSn} refers to the relaxed lattice constant for $Ge_{1-y}Sn_y$ at a given Sn concentration, and GeSn refers to the actual $Ge_{1-y}Sn_y$ epilayer grown and its HR-XRD ω–2θ coupled scan and RSMs were collected.

In-plane and out-of-plane strain of grown $Ge_{1-y}Sn_y$ epilayers were calculated using Eqs. (1) and (2) and presented in Table 1. It is evident that the thickness of the $Ge_{1-y}Sn_y$ epilayer does not affect the in-plane or out-of-plane strain if the thickness is less than the h_c (~0.10 μm). However, when the thickness of the $Ge_{1-y}Sn_y$ epilayer exceeds h_c, the strain relaxation begins, and both the in-plane and out-of-plane strains

Table 1. Summary of effects of strain relaxation on the Sn concentration and growth rate of $Ge_{1-y}Sn_y$ epilayers grown at 260 °C and 500 Torr on Si (001) via a relaxed Ge-VS.

Thickness (nm)	In-plane strain (10^{-3})	Out-of-plane strain (10^{-3})	Average Sn content (at.%)	Average growth rate (nm/min)
29	−15.4	12.1	11.6	9.7
50	−15.6	12.2	11.6	10.0
79	−15.8	12.4	11.6	9.9
95	−15.6	12.3	11.6	9.5
128	−11.1	8.7	11.8	8.5
150	−9.8	7.7	12.2	7.5
	−9.3	7.3	12.5	

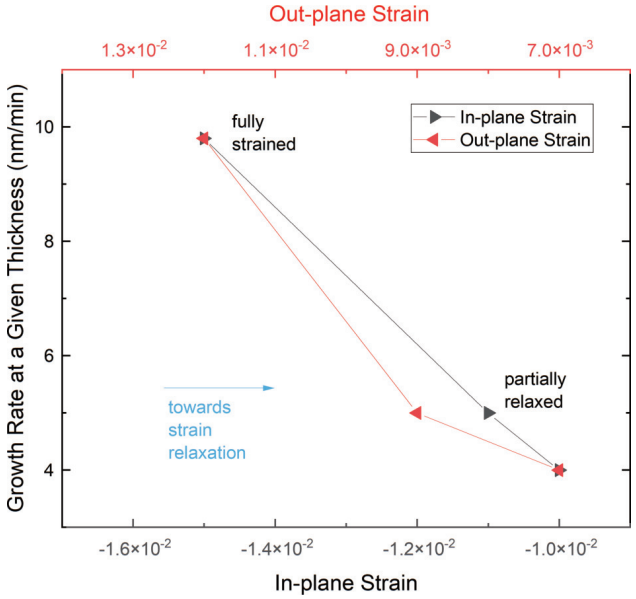

Fig. 5. (Colour online) The effect of strain relaxation in $Ge_{1-y}Sn_y$ epilayers on their growth rate. The growth rate at given strain relaxation state was estimated using the fitted line to the actual data points given in Fig. 4. In-plane and out-of-plane strain were calculated by Eqs. (1) and (2).

of the epilayer converge towards relaxed lattice constant, a_0^{GeSn}.

By considering the measured in-plane and out-of-plan strain, it is possible to investigate the effect of strain relaxation on both the growth rate and Sn concentration of $Ge_{1-y}Sn_y$ epilayers. As shown in Table 1, the average growth rate decreases as more strain relaxation are achieved. These average growth rates represent the growth rate for the entire $Ge_{1-y}Sn_y$ epilayers, not at a given in-plane or out-of-plane strain (or simply at a given thickness). To determine the true growth rate at a given thickness, the fitted line to the actual data shown in Fig. 4(b) can be used. Using this approach, the growth rate at a thickness of 128 nm was estimated to be ~5 nm/min and at a thickness of 150 nm was estimated to be ~4 nm/min. Based on these estimates, the effect of strain relaxation on the growth rate at given thicknesses can be explored. As shown in Fig. 5, the growth rate at the given thickness of the $Ge_{1-y}Sn_y$ epilayer is (almost) linearly dependent on the in-plane and out-of-plane strain. Since only two data points are available for partially relaxed $Ge_{1-y}Sn_y$, more studies are required to investigate further the effect of strain relax-

ation on the growth rate of the $Ge_{1-y}Sn_y$ epilayer at a given thickness.

As explained previously, the growth rate of $Ge_{1-y}Sn_y$ mainly depends on the Ge incorporation in the growing layers. Since all growth conditions such as temperature, pressure and partial pressures of precursors remained constant over the growth of all $Ge_{1-y}Sn_y$ epilayers, the production of Ge and Sn atoms remained constant. Therefore, the suppression of the Ge incorporation in growing layers cannot be due to the lack of Ge adatoms produced in the chamber. It seems that the strain relaxation directly influences the incorporation of Ge. As $Ge_{1-y}Sn_y$ relaxes more, a lower percentage of available Ge adatoms on the growing layers can be incorporated into the growing layers, resulting in a reduction in the growth rate.

Finally, the effect of strain relaxation on average Sn concentration can be examined. Here, we are discussing only the average Sn concentration across the entire $Ge_{1-y}Sn_y$ epilayer, rather than the Sn concentration at a specific thickness of the $Ge_{1-y}Sn_y$ epilayer. As shown in Table 1, the average Sn concentration increases as a result of strain relaxation. This can be explained by taking into account the effect of the growth rate on the average Sn concentration of $Ge_{1-y}Sn_y$ epilayers. Like Ge production, as CVD growth conditions remained the same, the production of Sn adatoms remained the same during the growth of $Ge_{1-y}Sn_y$ epilayer. Therefore, as the growth rate decreases, more of supplied Sn adatoms have the chance to incorporate into $Ge_{1-y}Sn_y$ growing layers, leading to an increase in Sn concentration.

It should be noted that even though the average growth rate decreases by ~55 % due decrease in incorporation of Ge into growing layers as a result of strain relaxation, the average Sn concentration in $Ge_{1-y}Sn_y$ has increased only by ~8 % from 11.6 at.% to 12.5 at.%. It is important to consider that this is the average Sn concentration of the whole epilayer and not just the top layers grown with lower growth rates. This result shows that the total Sn concentration does not significantly increase as a result of the reduction in growth rate, and the relationship could be nonlinear. This suggests that the incorporation rate of Sn into the growing $Ge_{1-y}Sn_y$ layers during the total growth time has indeed decreased, and the reason why the total Sn concentration is increased is because of the reduction in growth rate itself.

4. Conclusion

In this research, the effect of strain relaxation in compressive strained $Ge_{1-y}Sn_y$, which were grown at 260 °C, on growth rate is investigated. It is experimentally shown that strain relaxation within $Ge_{1-y}Sn_y$ decreases the growth rate of the epilayer. We also examined how Sn concentration and surface morphology of $Ge_{1-y}Sn_y$ epilayers may be influenced as a result of strain relaxation. It is important to note that strain relaxation could be potentially different in $Ge_{1-y}Sn_y$ epilayers with the same Sn concentration but grown under different CVD growth conditions. More experiments should be carried out to investigate strain relaxation for $Ge_{1-y}Sn_y$ epilayers grown under different CVD growth conditions. Furthermore, since the strain relaxation in $Ge_{1-y}Sn_y$ epilayers affects the electrical, for example indirect-to-direct bandgap transition[4, 23–27], and the physical properties of epilayers, it is therefore essential to consider further investigations in order to fully understand the mechanism of strain relaxation of $Ge_{1-y}Sn_y$ epilayers. This could pave the way for the widespread adoption of $Ge_{1-y}Sn_y$ based semiconductor devices and applications in the near future.

References

[1] Johnson E R, Christian S M. Some properties of germanium-silicon alloys. Phys Rev, 1954, 95, 560

[2] Göbel E O, Ploog K. Fabrication and optical properties of semiconductor quantum wells and superlattices. Prog Quantum Electron, 1990, 14, 289

[3] Joyce B A. Materials fundamentals of molecular beam epitaxy. Adv Mater, 1993, 5, 773

[4] Gupta S, Magyari-Köpe B, Nishi Y, et al. Achieving direct band gap in germanium through integration of Sn alloying and external strain. J Appl Phys, 2013, 113, 73707

[5] Wirths S, Buca D, Mantl S. Si–Ge–Sn alloys: From growth to applications. Prog Cryst Growth Charact Mater, 2016, 62, 1

[6] Lieten R R, Maeda T, Jevasuwan W, et al. Tensile-strained GeSn metal–oxide–semiconductor field-effect transistor devices on Si(111) using solid phase epitaxy. Appl Phys Express, 2013, 6, 101301

[7] Guo P F, Han G Q, Gong X, et al. $Ge_{0.97}Sn_{0.03}$ p-channel metal-oxide-semiconductor field-effect transistors: Impact of Si surface passivation layer thickness and post metal annealing. J Appl Phys, 2013, 114, 044510

[8] Eckhardt C, Hummer K, Kresse G. Indirect-to-direct gap transition in strained and unstrained Sn_xGe_{1-x} alloys. Phys Rev B, 2014, 89, 165201

[9] Zheng J, Liu Z, Xue C L, et al. Recent progress in GeSn growth and GeSn-based photonic devices. J Semicond, 2018, 39, 061006

[10] Oguz S, Paul W, Deutsch T F, et al. Synthesis of metastable, semiconducting Ge-Sn alloys by pulsed UV laser crystallization. Appl Phys Lett, 1983, 43, 848

[11] Soref R A, Friedman L. Direct-gap Ge/GeSn/Si and GeSn/Ge/Si heterostructures. Superlattices Microstruct, 1993, 14, 189

[12] Gurdal O, Desjardins P, Carlsson J R A, et al. Low-temperature growth and critical epitaxial thicknesses of fully strained metastable $Ge_{1-x}Sn_x$ ($x \leqslant 0.26$) alloys on $Ge(001)_2 \times 1$. J Appl Phys, 1998, 83, 162

[13] Mosleh A, Ghetmiri S A, Conley B R, et al. Material characterization of $Ge_{1-x}Sn_x$Alloys grown by a commercial CVD system for optoelectronic device applications. J Electron Mater, 2014, 43, 938

[14] Wang W, Zhou Q, Dong Y, et al. Critical thickness for strain relaxation of $Ge_{1-i>x}Sn_x$ ($x \leqslant 0.17$) grown by molecular beam epitaxy on Ge(001). Appl Phys Lett, 2015, 106, 232106

[15] Gencarelli F, Vincent B, Demeulemeester J, et al. Crystalline properties and strain relaxation mechanism of CVD grown GeSn. ECS J Solid State Sci Technol, 2013, 2, P134

[16] Bhargava N, Coppinger M, Prakash Gupta J, et al. Lattice constant and substitutional composition of GeSn alloys grown by molecular beam epitaxy. Appl Phys Lett, 2013, 103, 041908

[17] Takeuchi S, Sakai A, Yamamoto K, et al. Growth and structure evaluation of strain-relaxed $Ge_{1-x}Sn_x$ buffer layers grown on various types of substrates. Semicond Sci Technol, 2007, 22, S231

[18] Takeuchi S, Shimura Y, Nakatsuka O, et al. Growth of highly strain-relaxed $Ge_{1-x}Sn_x$/virtual Ge by a Sn precipitation controlled compositionally step-graded method. Appl Phys Lett, 2008, 92, 231916

[19] Takeuchi S, Sakai A, Nakatsuka O, et al. Tensile strained Ge layers on strain-relaxed $Ge_{1-x}Sn_x$/virtual Ge substrates. Thin Solid Films, 2008, 517, 159

[20] Wirths S, Tiedemann A T, Ikonic Z, et al. Band engineering and growth of tensile strained Ge/(Si)GeSn heterostructures for tunnel field effect transistors. Appl Phys Lett, 2013, 102, 192103

[21] Weisshaupt D, Jahandar P, Colston G, et al. Impact of Sn segregation on $Ge_{1-x}Sn_x$ epi-layers growth by RP-CVD. 2017 40th International Convention on Information and Communication Technology, Electronics and Microelectronics (MIPRO), 2017, 43

[22] Jahandar P, Weisshaupt D, Colston G, et al. The effect of Ge precursor on the heteroepitaxy of $Ge_{1-x}Sn_x$ epilayers on a Si (001) substrate. Semicond Sci Technol, 2018, 33, 034003

[23] Lu Low K, Yang Y, Han G Q, et al. Electronic band structure and effective mass parameters of $Ge_{1-x}Sn_x$ alloys. J Appl Phys, 2012, 112, 103106

[24] Tonkikh A A, Eisenschmidt C, Talalaev V G, et al. Pseudomorphic GeSn/Ge(001) quantum wells: Examining indirect band gap bowing. Appl Phys Lett, 2013, 103, 032106

[25] Dutt B, Lin H, Sukhdeo D S, et al. Theoretical analysis of GeSn alloys as a gain medium for a Si-compatible laser. IEEE J Sel Top Quantum Electron, 2013, 19, 1502706

[26] Ionescu A M, Riel H. Tunnel field-effect transistors as energy-efficient electronic switches. Nature, 2011, 479, 329

[27] Kotlyar R, Avci U E, Cea S, et al. Bandgap engineering of group IV materials for complementary n and p tunneling field effect transistors. Appl Phys Lett, 2013, 102, 113106

[28] Olesinski R W, Abbaschian G J. The Ge–Sn (Germanium–Tin) system. Bull Alloy Phase Diagr, 1984, 5, 265

[29] Fleurial J P, Borshchevsky A. Si-Ge-metal ternary phase diagram calculations. J Electrochem Soc, 1990, 137, 2928

[30] Zaima S, Nakatsuka O, Taoka N, et al. Growth and applications of GeSn-related Group-IV semiconductor materials. Sci Technol Adv Mater, 2015, 16, 043502

Pedram Jahandar earned his PhD from the University of Warwick after obtaining his Bachelor of Science and Master of Science degrees from King's College London. He specialises in Group Ⅳ semiconductor CVD epitaxy and device fabrication, and actively applies the latest technological advancements and academic achievements across various industries.